Journal of Magnetic Resonance 306 (2019) 118–123

Contents lists available at ScienceDirect

Journal of Magnetic Resonance

journal homepage: www.elsevier.com/locate/jmr

MR to go

J. Anders [a,*], K. Lips [b]

[a] University of Stuttgart, Institute of Smart Sensors and IQ^ST (Center for Integrated Quantum Science and Technology), Stuttgart, Germany
[b] Helmholtz-Zentrum Berlin für Materialien und Energie, Berlin Joint EPR Lab, Institute Nanospectroscopy, Berlin, Germany

ARTICLE INFO

Article history:
Received 18 February 2019
Revised 2 June 2019
Accepted 8 July 2019
Available online 9 July 2019

Keywords:
MR to go
MR-on-a-chip
NMR-on-a-chip
EPR-on-a-chip
VCO-based EPR
Portable MR spectrometers

ABSTRACT

In this paper, we provide a review of the recent advances in miniaturizing nuclear magnetic resonance (NMR) and electron paramagnetic resonance (EPR) spectrometers for portable magnetic resonance (MR) applications. We focus the discussion on the application of integrated circuit technology for the miniaturization of the NMR and EPR spectrometer hardware and/or the detector and we will briefly touch on magnet technology. Finally, we will summarize current challenges of chip-integrated spectrometers and give an outlook on future applications of mobile MR spectrometers.

1. Introduction

Magnetic resonance (MR) based methods are amongst the most powerful analytical techniques available today. Thanks to their unsurpassed specificity and complete non-invasiveness, nuclear magnetic resonance (NMR) spectroscopy and imaging continue to revolutionize analytical chemistry [1,2] and medical imaging [2,3]. Additionally, electron paramagnetic resonance (EPR) spectroscopy is recently gaining significant attention in both life science and material science applications due to e.g. the possibility of in-cell EPR experiments [4] and its ability of directly detecting free radicals, which play a major role in many diseases and which can cause premature cell aging [5–7]. Moreover, EPR is the prime modality for detecting paramagnetic defects in semiconductor and organic materials, rendering EPR a prime modality for the characterization of novel materials and devices [8,9].

Conventional high-end NMR and EPR equipment is bulky and expensive, making use of large B_0-field strengths to overcome the relatively poor sensitivity of inductively detected MR experiments. Therefore, the applicability of operando MR techniques with conventional equipment is drastically limited. However, to make the great analytical power of MR-based techniques available to a broader application range, there have been significant research efforts over the past ten to fifteen years to miniaturize the spectrometer size, cost and weight [10–25].

In this paper, we will review the recent advances in the so-called MR-on-a-chip approach, in which the spectrometer electronics and sometimes also the detection coil, are integrated into a single integrated circuit. More specifically, after a general introduction into the most salient features of and the possibilities associated with the MR-on-a-chip technology in Section 2, we will take a closer look at the state of the art of NMR-on-a-chip and VCO-based EPR-on-a-chip detectors in Sections 2.1 and 2.2, respectively. In this discussion, our focus will be to highlight the new features of the MR-on-a-chip approach compared to conventional MR detection that render the MR-on-a-chip approach a key enabler for future portable MR applications, but we will also discuss the limitations of existing realizations. In Section 3, we will conclude our paper with an outlook on potential future applications of portable MR devices enabled by the MR-on-a-chip approach.

2. MR-on-a-chip technology

To explain the general advantage of CMOS integrated MR hardware, Fig. 1 shows the cross section of a generic CMOS process. Here, the active devices (transistors) reside in a thin layer of epitaxially grown silicon and a relatively large number of metal layers (typically between five and ten) allow for a dense interconnection of the active devices. In addition, the metalization layers can be used to form passive devices such as capacitors and inductors. According to Fig. 1, especially the thick top metal layers with metal thicknesses between 1 μm and 4 μm together with the very good lateral resolution of the process allow for the realization of

* Corresponding author.
E-mail addresses: jens.anders@iis.uni-stuttgart.de (J. Anders), lips@helmholtz-berlin.de (K. Lips).

https://doi.org/10.1016/j.jmr.2019.07.007
1090-7807/

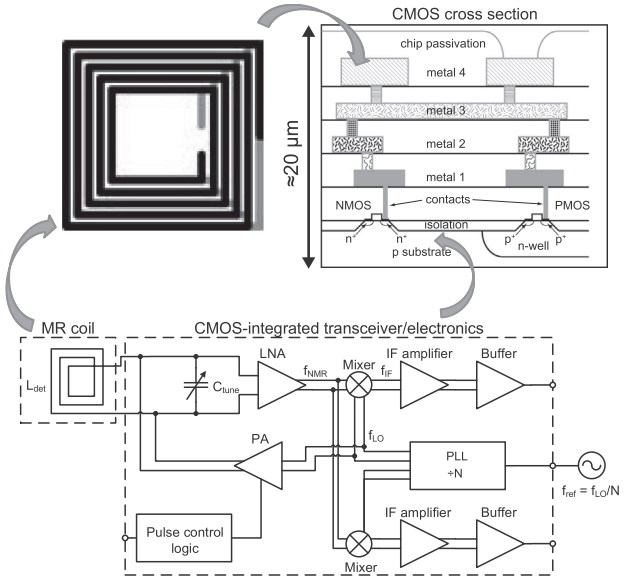

Fig. 1. Illustration of the fully-integrated MR-on-a-chip approach, in which the MR transceiver electronics and the detection coil are monolithically implemented in a single integrated circuit.

miniaturized coil designs with inner diameters down to ≈ 30 µm.[1] Therefore, the CMOS-integrated approach is well suited for the realization of on-chip MR detection coils with moderate quality factors between ten and 30 up to very high frequencies. The chip surface is typically passivated using silicon nitride and openings in the passivation layer allow for an electrical connection via bondwires. Since the total thickness of the layer stack is in general not exceeding 20 µm, the connection distance between an on-chip coil and the active electronics is only a very small fraction of the wavelength up to very high frequencies beyond 100 GHz. This short connection distance can be exploited by recalling that in an inductively detected MR experiment, the transceiver electronics serve two main purposes: In the receive path (RX path), the electronics have to amplify and frequency downconvert the MR-induced electromotive force (emf) in the coil. In the transmit path (TX path), the power amplifier (PA) has to deliver a sufficiently large current into the coil such that the B_1-field becomes sufficiently strong to produce acceptable flip angles within reasonably short pulse lengths. In a classical approach, where the electronics are located outside the B_0-field, the connection distance is typically a significant fraction of the wavelength, requiring impedance matched, transmission line based connections, which impose a certain impedance level – mostly 50 Ω – on the LNA and the PA, greatly limiting the design flexibility. In contrast, in a monolithic realization of the MR spectrometer, which co-integrates both the MR detection coil and the transceiver electronics, both for NMR and EPR frequencies, the LNA can be realized as a simple voltage LNA, reading out the MR-induced emf. Moreover, the power amplifier can in principle be designed as a current output PA, which can greatly simplify the complexity of the electronics and lead to reduced power consumptions in the MR transceiver electronics [26–28]. The latter two advantages make CMOS-integrated MR hardware particularly attractive because they allow for the realization of affordable spectrometer electronics with tiny footprints down to a few square millimeters. Nevertheless, such on chip spectrometers achieve a state of the art performance, which is comparable to and sometimes even better than bulky and costly high-end MR hardware.

[1] Not limited by the lithographic resolution but rather by the proximity effect, which makes the coil resistance increase rapidly for too small inner coil diameters.

Before splitting our discussion into two separate tracks for NMR- and EPR-on-a-chip detectors, we would like to say a few words about the general applicability of the MR-on-a-chip approach: It is a well-known fact that any MR sensor can be optimized for the two contradicting design goals of spin limited samples on the one hand and concentration limited samples on the other hand. With the possibility to manufacture highly miniaturized on-chip detection coils, the fully-integrated MR-on-a-chip approach is intrinsically ideally suited for high-sensitivity measurements on mass/spin limited samples such as single cells in in-cell NMR or EPR or measurements on small crystals. When striving for a good concentration sensitivity, it is in general advisable to maximize the detector volume. Within the framework of the MR-on-a-chip approach, this can be achieved in three different ways: A straightforward approach would be to use a conventional large scale detector in combination with the chip-integrated transceiver electronics. In this approach, one can benefit from the improved form factor of the miniaturized spectrometer electronics, but – depending on the coil/resonator size and/or the desired operating frequency – it might be hard to achieve the required power levels with the miniaturized electronics. In a second approach, one can combine the beneficial features of the MR-on-a-chip approach with external miniaturized detectors. If the external detectors are also manufacturable in a scalable technology such as MEMS type processes, the scalability of the MR-on-a-chip approach can be used to increase the sensitive volume by using a large number of detectors in an array configuration [29]. Thanks to the excellent scalability of MEMS-based detectors and the MR-on-a-chip electronics in combination with the improved spin sensitivity of the individual smaller-size detectors, in principle, very good concentration sensitivities can be realized using this method. Finally, in applications that can tolerate the somewhat inferior properties of a planar on-chip coil, the array-based approach can also be applied to fully-integrated MR-on-a-chip systems. Here, the upper limit of the number of array channels is mostly given by the silicon area and/or the heat generation of the array.

2.1. NMR-on-a-chip detectors

In the field of NMR, the possibilities of IC-based realizations have mainly been used to monolithically integrate the NMR spectrometer electronics of Fig. 1, while the NMR detection coil is typically realized off-chip to meet the stringent requirements on its B_1-field homogeneity and coil-induced susceptibility artifacts. Therefore, the actual detection principle of the NMR-on-a-chip approach largely remains the same as in conventional NMR, the main difference being the small form factor and the close proximity of the NMR electronics to the coil, which together enable larger degrees of freedom in the overall system design.

One prototype system that uses the combination of a monolithically integrated NMR-on-a-chip transceiver and an external coil for true NMR spectroscopy has been presented in [14], cf. Fig. 2a. In this system the required B_0-field homogeneity has been achieved by the combination of a permanent magnet and electrical shim coils. The presented NMR-on-a-chip transceiver makes full use of the close proximity between the NMR coil and the transceiver chip by avoiding a 50Ω matching to fully exploit the noise-free preamplification from the tuning capacitance. This noise free preamplification amplifies both the induced NMR signal and the voltage noise produced by the coil[2] by the quality factor of the LC resonant tank, which is typically dominated by the coil quality factor. Thereby, the burden on the input referred voltage noise of the LNA is greatly relaxed. Finally, the ^{1}H-^{13}C-heteronuclear NMR

[2] And the sample.

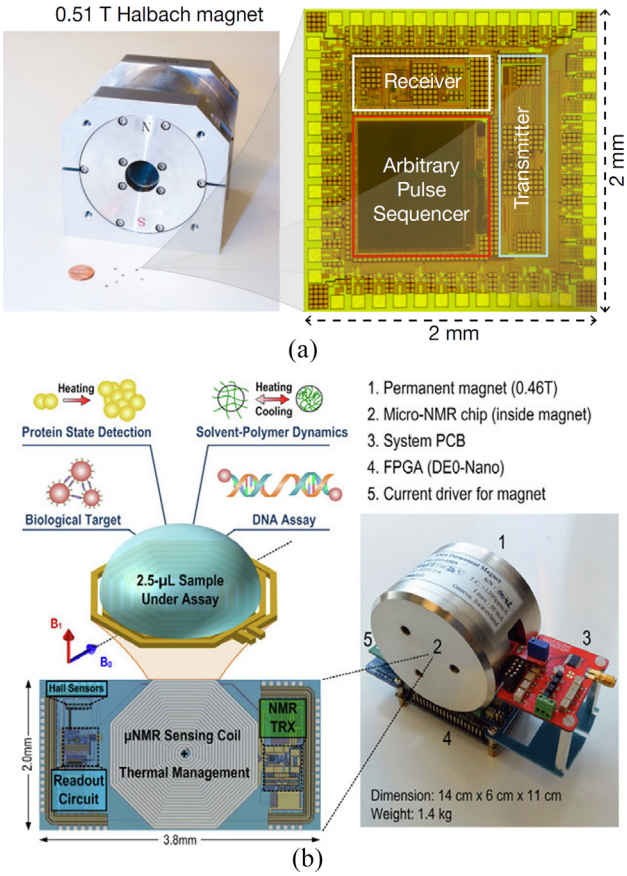

Fig. 2. (a) Photograph and micrograph of the portable NMR system and the utilized ASIC presented in [14], graphic taken from [14] and (b) photograph, micrograph and concept drawing of the point-of-care NMR-system, the utilized ASIC and the target application presented in [30], graphic taken from [30].

experiments presented in [14], which used two transceiver chips for the two hardware channels, clearly demonstrate the versatility of the NMR-on-a-chip approach.

As a second example of the rich possibilities associated with the NMR-on-a-chip approach, in [30], a portable NMR relaxometry system has been presented. It uses a co-integrated Hall sensor to measure B_0-field fluctuations, which are then compensated by an auxiliary coil. Moreover, in this setup, the on-chip NMR coil – due to the target relaxometry application the inferior B_1-field homogeneity and susceptibility artifacts are tolerable in this design – has been re-used in combination with an on-chip temperature sensor for the stabilization of the sample temperature against environmental fluctuations. Overall, the system presented in [30] nicely illustrated the added design freedom by the NMR-on-a-chip approach that allows to augment the core NMR system by auxiliary sensors that can be used to enhance the performance of the NMR unit.

A second example of a fully-integrated NMR-on-a-chip transceivers with co-integrated detection coil is the design in [13], which uses the miniaturized on-chip broadband NMR coil for single-cell NMR spectroscopy experiments. The broadband NMR approach presented in this paper is particularly interesting because it fully exploits the freedom of co-designing the NMR coil together with the transceiver electronics. As discussed e.g. in [31,27], the intrinsic coil SNR is a very mild function of the coil geometry, leading to a situation where coils with many turns and moderate quality factors display very similar SNR values as single turn, high-Q saddle coils as they are frequently used in conventional NMR spectroscopy. In [13], this design freedom was used to create an on-chip NMR coil with a very large AC resistance. The large intrinsic coil noise – here it should be stressed that the intrinsic coil SNR was still very competitive due to the large induced voltage in the multi turn design – then allowed for the design of a broadband COMS LNA, whose input referred voltage noise was significantly below the coil noise, i.e. which provided a very good noise figure.

As already briefly mentioned above, the scalability of the NMR-on-a-chip transceiver electronics in principle allows for the realization of large scale arrays of miniaturized detection coils that enable both an excellent spin sensitivity and at the same time a good concentration sensitivity. A smaller scale example of such a system consisting of MEMS-based, miniaturized 3D solenoidal NMR coils and custom designed receiver electronics was presented in [29].

An interesting feature of systems using an in-field preamplifier is the possibility of using an electronically controllable varactor to form an adjustable parallel LC resonant circuit with the detection coil that performs the abovementioned noise free preamplification. This simplified tuning scheme was used in [32] for multinuclear (X-nuclei) magnetic resonance imaging (MRI) experiments with a greatly simplified setup compared to conventional multituned coils. In this paper, it was experimentally demonstrated that the use of in-field electronics next to a conventional MRI coil removes the need for an impedance match between the coil and the LNA even for large, centimeter-sized coils, thereby greatly facilitating X-nuclei MRI experiments when using an electronically tunable capacitor for the tuning.

2.2. VCO-based EPR-on-a-chip detectors

As mentioned above, due ot the very stringent requirements on the B_0- and B_1-field homogeneity in NMR, most IC-based NMR spectrometry systems use an external coil in combination with a CMOS in-field transceiver. In contrast, the relaxed requirements on the field homogeneity in EPR allow for an even more aggressive integration approach, in which the detection coil is co-integrated on the same ASIC without performance loss. Another important difference between chip-integrated NMR and EPR transceiver results from the fact that today – due to hardware limitations – most EPR experiments are still carried out in the continuous-wave regime.

The architecture of a conventional, resonator-based EPR experiment is illustrated in Fig. 3a, where the elements that prevent a straightforward miniaturization of the setup are highlighted in red. Here, it is mostly the electromagnet, which imposes an overall large system size, weight and power consumption. The electromagnet is required because the conventional mechanically tuned volume resonators used in EPR are mostly incompatible with frequency sweep experiments. This is because it is difficult to readjust their tuning at every sweep point and, therefore, the resonators introduce a hard tradeoff between Q-factor, sweep range and sensitivity variations over the sweep range. As a solution to this problem, in [20], the voltage-controlled oscillator (VCO) based EPR detection approach, which is illustrated in Fig. 3b, has been proposed as an extension to the previously proposed oscillator-based EPR approach [33–37]. The oscillator based approach with its miniaturized detection coils and (fundamental) operation frequencies up to 150 GHz was mainly aiming at improving the spin sensitivity and room temperature sensitivities as good as 2×10^7 spins/$\sqrt{\text{Hz}}$ at 150 GHz have been presented [37]. Interestingly, the chip-integrated oscillators also display a very good performance down to cryogenic temperatures and operations down to 1.4 K using high electron mobility transistors have already been presented in the literature [38].

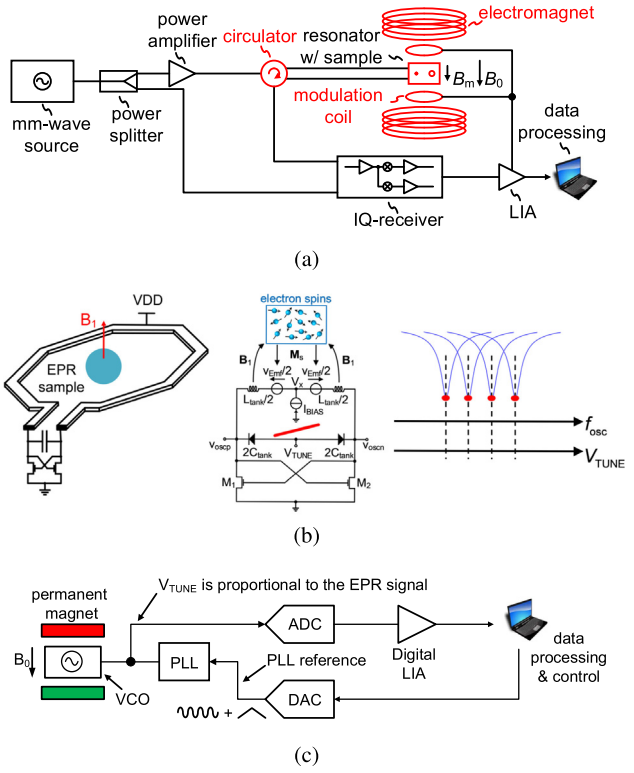

Fig. 3. (a) Conventional resonator-based EPR detection setup with the components that prevent a straightforward miniaturization of the setup highlighted in red, (b) illustration of the VCO-based EPR detection approach and (c) experimental setup of the VCO-based detection method. (For interpretation of the references to color in this figure legend, the reader is referred to the web version of this article.)

In the VCO-based approach, the EPR sample is placed on top of the coil of an integrated VCO. The B_1-field necessary to excite the spin ensemble is produced by the current running in the coil and the EPR signal is detected as a change of the oscillation amplitude and frequency produced by the spin-induced emf in the coil. The VCO can be realized in many different ways, but a particularly suitable realization for CMOS integration is the crosscoupled pair LC tank oscillator shown in Fig. 3b, which is in essence an LC resonator coupled to a crosscoupled transistor pair. Here, the crosscoupled transistor pair replenishes the loss of the LC tank resonator, producing a stable oscillation at[3] the LC tank resonance frequency $\omega_{LC} = \sqrt{1/(L_{tank}C_{tank})}$. In a VCO, the tank capacitance is realized as an electrically tunable capacitor, whose value depends on a tuning voltage V_{TUNE}, i.e. $C_{tank} = C_{tank}(V_{TUNE})$. Thereby, the operating frequency of the VCO can be readily adjusted by changing $C_{tank}(V_{TUNE})$ via said tuning voltage. Here, according to Fig. 3b, changing V_{TUNE} not only changes the operating frequency but also the resonance frequency of the LC tank resonator embedded inside the VCO. Therefore, when performing frequency sweeps by changing V_{TUNE}, the LC resonator inside the VCO is at each sweep point critically coupled to the frequency of the B_1-field, leading to very small[4] sensitivity variations even for very wide frequency sweeps. Thereby, the VCO-based detection approach opens up the path towards portable EPR spectrometers according to Fig. 3c, which use a permanent magnet as source for the static B_0-field. A photograph of the latest prototype of a battery-operated, portable EPR spectrometer manufactured in Stuttgart, which is an improved version of the spectrometer presented in [20], is shown in Fig. 4. Interestingly, the VCO-based detector can be incorporated into a phase-locked loop (PLL), which causes the VCO frequency to be equal to a multiple of the PLL reference [39]. Thereby, the frequency of the B_1-field is precisely defined by the external reference and the EPR-induced frequency shift is translated into a corresponding change of the VCO tuning voltage. When using a source with frequency modulation capabilities as the PLL reference, the reference signal can also be used to generate the frequency modulation required for lock-in detection. In the resulting PLL-based spectrometer architecture shown in Fig. 3c, the EPR signal is contained in the tuning voltage such that the lock-in amplifier can be directly connected to V_{TUNE}, leading to a very simple all-electronic, overall system architecture that can be easily integrated into standard CMOS.

As an important difference to conventional resonator-based EPR, in the VCO-based approach, the EPR-induced frequency signal is proportional to the real part of the complex susceptibility, leading to dispersion type EPR spectral lines, cf. [28]. However, the amplitude of the VCO is also affected by the EPR effect, where one can show that the EPR-induced amplitude shift is mostly proportional to the imaginary part of the complex sample susceptibility [31], producing the conventional absorption type EPR spectra in this detection mode of the VCO-based sensor.

Interestingly, despite the potential increase in the VCO noise compared to a fixed frequency oscillator due to the AM/PM conversion in the varactor, the spin sensitivities with the VCO-based systems presented in [39] are equal in the frequency sweep mode and the field sweep mode[5] and the system of [39] achieved a spin sensitivity around $10^9 \text{spins}/\sqrt{\text{Hz}}$ at 14 GHz.

When initially proposed in [20], one major limitation of the CMOS-integrated VCO-based approach was the limited maximum size of the integrated detection coils – depending on the operating frequency, between a few tens of microns to a few hundred microns – which greatly limited the achievable concentration sensitivity. As a solution to this problem, in [21], the VCO-based detection approach was extended to arrays of injection locked VCOs. In this approach, all VCOs are electrically coupled to synchronize their oscillation phase,[6] cf. Fig. 5a. In this way, the sensitive volume can be improved by increasing the number of coupled oscillators. For a homogeneous sample covering the entire VCO array according to Fig. 5b, the sensitivity, i.e. the EPR-induced frequency change per spin, is unaltered compared to the frequency change per spin of a single array element. Hence, the concentration sensitivity improves linearly with the number of array channels, N_{VCO}, due to the increased volume [21]. Since the white noise floor of the joint array frequency improves with $\sqrt{N_{VCO}}$ compared to a single array element, overall, the concentration sensitivity of an array of N_{VCO} identical VCOs displays a $N_{VCO}^{3/2}$-fold improved concentration sensitivity compared to an individual VCO. As a result, the design presented in [21] achieved a concentration sensitivity of 200 μM at 14 GHz, which was roughly ten times improved compared to a single element of the VCO array.

One major advantage of the VCO-based detector array compared to an array of resonators is the fact that, in the VCO array case, the readout complexity is independent of the number of array channels because the EPR signal is contained in the joint array frequency. Therefore, only a single signal has to be read out for an array of phase-locked VCO-based EPR detectors, whereas in the case of an array of resonators, each channel in principle requires its own transceiver, greatly increasing the excitation and readout complexity for large array channel counts.

[3] More precisely near.
[4] There are some residual sensitivity variations due to the slightly nonlinear relation between C_{tank} and V_{TUNE}.
[5] That uses a highly stabilized and low-nosie tuning voltage.
[6] And therefore also their oscillation frequency.

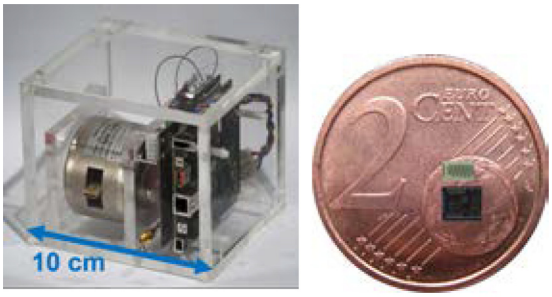

Fig. 4. (a) Photograph of the latest prototype of our battery-operated, portable EPR spectrometers using the VCO-based operating principle introduced by our group in [20] and (b) micrographs of EPR-on-a-chip and an NMR-on-a-chip ASICs (EPR above, NMR below) in size comparison to a two cent coin.

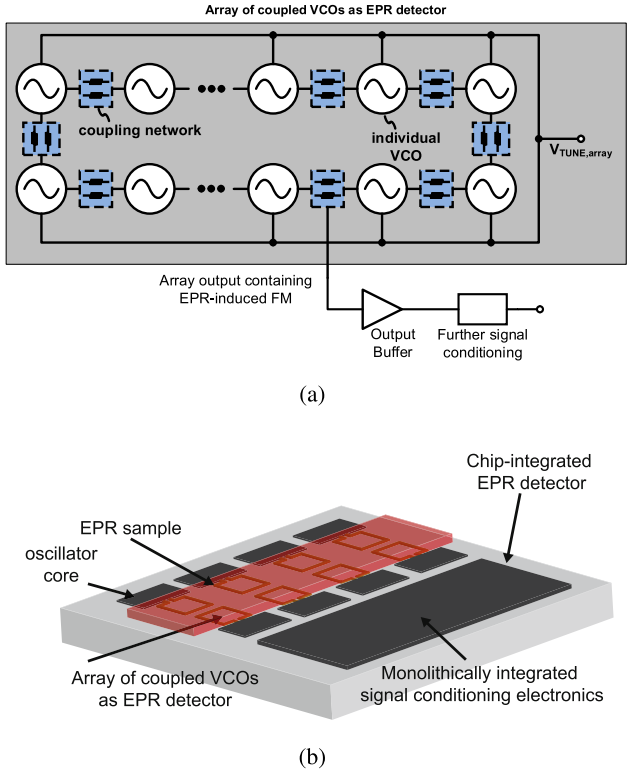

Fig. 5. (a) Conceptual schematic of an array of injection-locked VCO-based EPR detectors and (b) conceptual view of a monolithically integrated injection locked EPR detector array including sample placement.

Overall, arrays of injection-locked VCO-based EPR detectors provide a very promising way towards cheap, yet high performance EPR detectors even up to very high frequencies beyond 100 GHz. Since the VCO arrays inherit all the positive system aspects of single-element VCOs – constant sensitivity frequency sweeps, embeddability into a PLL for a precise frequency definition of the B_1-frequency from an external reference – the injection-locked VCO arrays appear to present an ideal platform for future generations of portable EPR spectrometers.

3. Conclusions and outlook

In this paper, we have discussed the possibilities associated with the use of IC technologies for the monolithic integration of MR spectrometer electronics and detection coils. We have explained how the basic features of modern IC technologies such as CMOS can not only be used for a miniaturized realization of conventional MR transceiver systems but that the in-field electronics together with the very short electrical connections can be used to realize more efficient transceiver architectures that directly reflect the nature of the MR excitation and detection signals. These new architectures are therefore ideally suited for the realization of future miniaturized, cheap, power-efficient, yet high-performance MR spectrometers. In the field of EPR, we have then discussed in detail the recently proposed VCO-based EPR detection approach, including the use of injection-locked VCO arrays. Especially these arrays, which combine both the detector and the required signal conditioning electronics into a tiny chip of a few square millimeters bear the potential to revolutionize the field of EPR spectroscopy. Combined with the recent advances in magnet technology, which allow to realize very homogeneous magnets with continuously decreasing size, cf. [22–25], the MR-on-a-chip technology might turn the dream of an MR spectrometer with the form factor as small as that of a conventional smart phone into a reality. Such portable MR devices could then find wide usage in a broad range of applications including MR-based quality monitoring in the context of Industry 4.0 and MR-based personalized medicine.

References

[1] C.D. Huang, P. Rossi, T. Saio, C.G. Kalodimos, Structural basis for the antifolding activity of a molecular chaperone, Nature 537 (7619) (2016) 202, https://doi.org/10.1038/nature18965, URL: <Go to ISI>://WOS:000382539100041.
[2] S.J. DeVience, L.M. Pham, I. Lovchinsky, A.O. Sushkov, N. Bar-Gill, C. Belthangady, F. Casola, M. Corbett, H.L. Zhang, M. Lukin, H. Park, A. Yacoby, R.L. Walsworth, Nanoscale nmr spectroscopy and imaging of multiple nuclear species, Nat. Nanotechnol. 10 (2) (2015) 129–134, https://doi.org/10.1038/nnano.2014.313, URL: <Go to ISI>://WOS:000349468200010.
[3] J.H. Lee, S.Y. Baek, Y. Song, S. Lim, H. Lee, M.P. Nguyen, E.J. Kim, G.Y. Huh, S.Y. Chun, H. Cho, The neuromelanin-related t-2* contrast in postmortem human substantia nigra with 7t mri, Sci. Rep. 6 (2016), https://doi.org/10.1038/srep32647, ARTN 32647. URL: <Go to ISI>://WOS:000382464500001.
[4] M. Azarkh, V. Singh, O. Oklre, I.T. Seemann, D.R. Dietrich, J.S. Hartig, M. Drescher, Site-directed spin-labeling of nucleotides and the use of in-cell epr to determine long-range distances in a biologically relevant environment, Nat. Protoc. 8 (1) (2013) 131–147, https://doi.org/10.1038/nprot.2012.136, URL: <Go to ISI>://WOS:000313051300010.
[5] E. Piskounova, M. Agathocleous, M.M. Murphy, Z.P. Hu, S.E. Huddlestun, Z.Y. Zhao, A.M. Leitch, T.M. Johnson, R.J. DeBerardinis, S.J. Morrison, Oxidative stress inhibits distant metastasis by human melanoma cells, Nature 527 (7577) (2015) 186, https://doi.org/10.1038/nature15726, URL: <Go to ISI>://WOS:000364396700035.
[6] M.T. Lin, M.F. Beal, Mitochondrial dysfunction and oxidative stress in neurodegenerative diseases, Nature 443 (7113) (2006) 787–795, https://doi.org/10.1038/nature05292, URL: <Go to ISI>://WOS:000241362700038.
[7] M. Kopani, P. Celec, L. Danisovic, P. Michalka, C. Biro, Oxidative stress and electron spin resonance, Clin. Chim. Acta 364 (1–2) (2006) 61–66, https://doi.org/10.1016/j.cca.2005.05.016, URL: <Go to ISI>://WOS:000235376800005.
[8] X.J. Wang, I.A. Buyanova, F. Zhao, D. Lagarde, A. Balocchi, X. Marie, C.W. Tu, J.C. Harmand, W.M. Chen, Room-temperature defect-engineered spin filter based on a non-magnetic semiconductor, Nat. Mater. 8 (3) (2009) 198–202, https://doi.org/10.1038/Nmat2385, URL: <Go to ISI>://WOS:000263556800017.
[9] K. Kang, S. Watanabe, K. Broch, A. Sepe, A. Brown, I. Nasrallah, M. Nikolka, Z.P. Fei, M. Heeney, D. Matsumoto, K. Marumoto, H. Tanaka, S. Kuroda, H. Sirringhaus, 2d coherent charge transport in highly ordered conducting polymers doped by solid state diffusion, Nat. Mater. 15 (8) (2016) 896, https://doi.org/10.1038/Nmat4634, URL: <Go to ISI>://WOS:000380849200025.
[10] J. Anders, J. Handwerker, M. Ortmanns, G. Boero, A low-power high-sensitivity single-chip receiver for nmr microscopy, J. Magn. Reson. 266 (2016) 41–50, https://doi.org/10.1016/j.jmr.2016.03.004, URL: <Go to ISI>://WOS:000375510100005.
[11] E. Danieli, J. Perlo, B. Blumich, F. Casanova, Small magnets for portable nmr spectrometers, Angew. Chem. Int. Ed. 49 (24) (2010) 4133–4135, https://doi.org/10.1002/anie.201000221, URL: <Go to ISI>://WOS:000278796400028.
[12] M. Grisi, G.M. Conley, P. Sommer, J. Tinembart, G. Boero, A single-chip integrated transceiver for high field nmr magnetometry, Rev. Sci. Instrum. 90 (1) (2019) 015001, https://doi.org/10.1063/1.5066436.
[13] M. Grisi, F. Vincent, B. Volpe, R. Guidetti, N. Harris, A. Beck, G. Boero, Nmr spectroscopy of single sub-nl ova with inductive ultra-compact single-chip probes, Sci. Rep. 7 (2017), https://doi.org/10.1038/srep44670, ARTN 44670. URL: <Go to ISI>://WOS:000396667400001.

[14] D. Ha, J. Paulsen, N. Sun, Y.Q. Song, D. Ham, Scalable nmr spectroscopy with semiconductor chips, Proc. Natl. Acad. Sci. USA 111 (33) (2014) 11955–11960, https://doi.org/10.1073/pnas.1402015111, URL: <Go to ISI>://WOS:000340438800029.
[15] A. Haber, B. Blumich, D. Souvorova, E. Del Federico, Ancient roman wall paintings mapped nondestructively by portable nmr, Anal. Bioanal. Chem. 401 (4) (2011) 1441–1452, https://doi.org/10.1007/s00216-011-5180-3, URL: <Go to ISI>://WOS:000293632700038.
[16] R. Haken, B. Blumich, Anisotropy in tendon investigated in vivo by a portable nmr scanner, the nmr-mouse, J. Magn. Reson. 144 (2) (2000) 195–199, https://doi.org/10.1006/jmre.2000.2040, URL: <Go to ISI>://WOS:000087523700002.
[17] J. Perlo, V. Demas, F. Casanova, C.A. Meriles, J. Reimer, A. Pines, B. Blumich, High-resolution nmr spectroscopy with a portable single-sided sensor, Science 308 (5726) (2005) 1279, https://doi.org/10.1126/science.1108944, URL: <Go to ISI>://WOS:000229482300037.
[18] N. Sun, T.J. Yoon, H. Lee, W. Andress, R. Weissleder, D. Ham, Palm nmr and 1-chip nmr, IEEE J. Solid-State Circ. 46 (1) (2011) 342–352, https://doi.org/10.1109/Jssc.2010.2074630, URL: <Go to ISI>://WOS:000285839200030.
[19] J. Handwerker, M. Eder, M. Tibiletti, V. Rasche, K. Scheffler, J. Becker, M. Ortmanns, J. Anders, An array of fully-integrated quadrature tx/rx nmr field probes for mri trajectory mapping, in: ESSCIRC, 2016, pp. 217–220, https://doi.org/10.1109/ESSCIRC.2016.7598281.
[20] J. Handwerker, B. Schlecker, U. Wachter, P. Radermacher, M. Ortmanns, J. Anders, A 14ghz battery-operated point-of-care esr spectrometer based on a 0.13 m cmos asic, in: IEEE International Solid-State Circuits Conference (ISSCC) , 2016, pp. 476–477, https://doi.org/10.1109/ISSCC.2016.7418114.
[21] A. Chu, B. Schlecker, K. Lips, M. Ortmanns, J. Anders, An 8-channel 13ghz esr-on-a-chip injection-locked vco-array achieving 200 m-concentration sensitivity, in: IEEE International Solid - State Circuits Conference – (ISSCC), 2018, pp. 354–356, https://doi.org/10.1109/ISSCC.2018.8310330.
[22] B. Blumich, Beyond compact nmr, Micropor. Mesopor. Mater. 269 (2018) 3–6, https://doi.org/10.1016/j.micromeso.2017.04.039, URL: <Go to ISI>://WOS:000438324000002.
[23] B. Blumich, K. Singh, Desktop nmr and its applications from materials science to organic chemistry, Angew. Chem. Int. Ed. 57 (24) (2018) 6996–7010, https://doi.org/10.1002/anie.201707084, URL: <Go to ISI>://WOS:000434350400004.
[24] C. Rehorn, B. Blumich, Cultural heritage studies with mobile nmr, Angew. Chem. Int. Ed. 57 (25) (2018) 7304–7312, https://doi.org/10.1002/anie.201713009, URL: <Go to ISI>://WOS:000434949200004.
[25] K. Singh, B. Blumich, Compact low-field nmr spectroscopy and chemometrics: a tool box for quality control of raw rubber, Polymer 141 (2018) 154–165, https://doi.org/10.1016/j.polymer.2018.02.057, URL: <Go to ISI>://WOS:000429484400017.
[26] J. Anders, Nonlinear Modeling of Continuous-Wave Spin Detection Using Oscillator-Based ESR-on-a-Chip Sensors, Springer International Publishing, 2018.
[27] J. Anders, A.H. Velders, Microcoils for broadband multinuclei detection, Micro Nano Scale NMR (2018), https://doi.org/10.1002/9783527697281 (Chapter 10).
[28] J. Handwerker, J. Anders, Ic-based and ic-assisted nmr detectors, Micro Nano Scale NMR (2018), https://doi.org/10.1002/9783527697281 (Chapter 6).
[29] V. Badilita, K. Kratt, N. Baxan, J. Anders, D. Elverfeldt, G. Boero, J. Hennig, J.G. Korvink, U. Wallrabe, 3d solenoidal microcoil arrays with cmos integrated amplifiers for parallel mr imaging and spectroscopy (2011) 809–812.
[30] K.-M. Lei, H. Heidari, P.-I. Mak, M.-K. Law, F. Maloberti, R.P. Martins, A handheld 50pm-sensitivity micro-nmr cmos platform with b-field stabilization for multi-type biological/chemical assays, in: Solid-State Circuits Conference (ISSCC), 2016 IEEE International, 2016.
[31] J. Anders, Fully-integrated cmos probes for magnetic resonance applications.
[32] A. Horneff, B. Schlecker, M. Hberle, E. Hell, J. Ulrici, V. Rasche, J. Anders, A new cmos broadband, high impedance lna for mri achieving an input referred voltage noise spectral density of 200pv/hzG (May 2019). doi: https://doi.org/10.1109/ISCAS.2019.8702445.
[33] T. Yalcin, G. Boero, Single-chip detector for electron spin resonance spectroscopy, Rev. Sci. Instrum. 79 (9) (2008), https://doi.org/10.1063/1.2969657, Artn 094105. URL: <Go to ISI>://WOS:000260291800041.
[34] J. Anders, A. Angerhofer, G. Boero, K-band single-chip electron spin resonance detector, J. Magn. Reson. 217 (2012) 19–26, https://doi.org/10.1016/j.jmr.2012.02.003, URL: <Go to ISI>://WOS:000303083500004.
[35] G. Boero, G. Gualco, R. Lisowski, J. Anders, D. Suter, J. Brugger, Room temperature strong coupling between a microwave oscillator and an ensemble of electron spins, J. Magn. Reson. 231 (2013) 133–140, https://doi.org/10.1016/j.jmr.2013.04.004, URL: <Go to ISI>://WOS:000319548300018.
[36] G. Gualco, J. Anders, A. Sienkiewicz, S. Alberti, L. Forro, G. Boero, Cryogenic single-chip electron spin resonance detector, J. Magn. Reson. 247 (2014) 96–103, https://doi.org/10.1016/j.jmr.2014.08.013, URL: <Go to ISI>://WOS:000343690900014.
[37] A.V. Matheoud, G. Gualco, M. Jeong, I. Zivkovic, J. Brugger, H.M. Ronnow, J. Anders, G. Boero, Single-chip electron spin resonance detectors operating at 50 ghz, 92 ghz, and 146 ghz, J. Magn. Reson. 278 (2017) 113–121, https://doi.org/10.1016/j.jmr.2017.03.013, URL: <Go to ISI>://WOS:000400723900013.
[38] A.V. Matheoud, N. Sahin, G. Boero, A single chip electron spin resonance detector based on a single high electron mobility transistor, J. Magn. Reson. 294 (2018) 59–70, https://doi.org/10.1016/j.jmr.2018.07.002, URL: http://www.sciencedirect.com/science/article/pii/S1090780718301733.
[39] B. Schlecker, A. Hoffmann, A. Chu, M. Ortmanns, K. Lips, J. Anders, Towards low-cost, high-sensitivity point-of-care diagnostics using vco-based esr-on-a-chip detectors, IEEE Sens. J. (2018) 1, https://doi.org/10.1109/JSEN.2018.2875767.